Accepted version. The final version is available at: DOI 10.1109/MMM.2016.2616180

The Beauty of Symmetry

Common-mode rejection filters for high-speed interconnects and balanced microwave circuits

[1]Ferran Martín, [1]Jordi Naqui, [2]Armando Fernández-Prieto, [1]Paris Vélez, [1]Jordi Bonache, [2]Jesús Martel, and [2]Francisco Medina

[1]CIMITEC, Departament d'Enginyeria Electrònica
Universitat Autònoma de Barcelona, 08193 Bellaterra (Barcelona), Spain
Corresponding author: Ferran.Martin@uab.es

[2]Grupo de Microondas,
Universidad de Sevilla. Avenida Reina Mercedes s/n, 41012 Sevilla, Spain.
E-mail: Medina@us.es

Common-mode rejection filters operating at microwave frequencies have been the subject of intensive research activity in the last decade. These filters are of interest for the suppression of common-mode noise in high-speed digital circuits, where differential signals are widely employed due to the high immunity to noise, electromagnetic interference (EMI) and crosstalk of differential-mode interconnects. These filters can also be used to improve common-mode rejection in microwave filters and circuits dealing with differential signals. Ideally, common-mode stopband filters should be transparent for the differential mode from DC up to very high frequencies (all-pass), should preserve the signal integrity for such mode, and should exhibit the widest and deepest possible rejection band for the common mode in the region of interest. Moreover, these characteristics should be achieved by means of structures with the smallest possible size. In this article, several techniques for the implementation of common-mode suppression filters in planar technology are reviewed. In all the cases, the strategy to simultaneously achieve common-mode suppression and all-pass behavior for the differential mode is based on selective mode-suppression. This selective mode suppression (either the common or the differential mode) in balanced lines is typically (although not exclusively) achieved by symmetrically loading the lines with symmetric resonant elements, opaque for the common-mode and transparent for the differential mode (common-mode suppression), or vice versa (differential-mode suppression).

SELECTIVE MODE SUPPRESSION IN BALANCED LINES

Let us review the general principle to achieve selective mode suppression (common mode or differential mode) in balanced lines through symmetric resonators (which is the

main approach considered in this article). It is well known that a transmission line (either single-ended or balanced) loaded with a resonator coupled to it exhibits a stop band (transmission zero, or notch) at the fundamental resonance frequency (and eventually at higher-order harmonics). Signal propagation is inhibited at these frequencies because the injected power is reflected back to the source. However, depending on the topology of the symmetric resonator and the relative orientation between the resonator and the line, it is possible to prevent the appearance of resonance (and hence the notch in the transmission coefficient) [1], [2].

Let us consider a symmetric line loaded with a symmetric resonator (coupled to it) with its symmetry plane perfectly aligned with the symmetry plane of the transmission line, so that the structure is perfectly symmetric with respect to the bi-section midplane. If the symmetry planes of the line (for the considered mode, i.e., common mode or differential mode) and resonator (for the considered resonance frequency, i.e., fundamental or higher-order harmonic) are of the same electromagnetic nature (either electric or magnetic walls), the resonator is excited, the structure is resonant, and signal propagation is inhibited in the vicinity of the considered resonance frequency. Conversely, if the symmetry plane of the line is an electric wall and the one of the resonator is a magnetic wall, or vice versa, the resonator cannot be excited. The reason is that, due to perfect symmetry, the net electric and magnetic field components "illuminating" the resonator exactly cancel (i.e., the electric and magnetic fluxes over the resonator area are zero) if the symmetry planes of line and resonator are of different nature. Under these conditions, the structure is all-pass, at least in the vicinity of the resonance frequency under consideration. If the symmetry planes of the line and resonator are misaligned, and both elements are close enough, line-to-resonator coupling activates, and the resulting notch depth in the transmission coefficient is determined by the level of misalignment (this idea has been exploited for the implementation of various types of sensors and detectors based on symmetry properties [3]-[8]).

For microstrip differential lines, either the common mode or the differential mode can be selectively suppressed while preserving the other mode unaltered (or almost unaltered) by aligning with the line a resonator exhibiting either a magnetic wall or an electric wall, respectively. This filtering functionality, referred to as selective mode suppression [9]-[11], is illustrated in Fig. 1(a) by considering a complementary split ring resonator (CSRR) [12] as a loading (coupled) element. Such a resonant element exhibits a magnetic wall at the fundamental resonance, and hence it inhibits signal propagation at that frequency for the common mode, whereas the line is transparent for the differential mode. Thus, CSRRs are useful for the implementation of common-mode suppression filters. Mode suppression can be reversed by loading the differential line, e.g., with split ring resonators (SRRs) [13] symmetrically placed at the upper metal level, between the pair of lines (Fig. 1b). The reason is that SRRs exhibit an electric wall at their symmetry plane at the fundamental resonance frequency [14],[15] (this resonator is the dual, or complementary, counterpart of the CSRR). The suppression of

the differential mode may be of interest in certain applications, but this differential mode suppression phenomenon is beyond the scope of this article, which is primarily focused on common-mode suppression filters. Many other resonant elements can be used for selectively suppressing the common mode in differential lines, including magnetic and electric LC resonators [11], dumbbell-shaped resonators [16], C-shaped resonators [17], and folded slotted stepped impedance resonators. The application of some of these resonant elements to the implementation of common-mode rejection filters is reviewed in the article, where, typically, several resonators are cascaded in order to enhance the common-mode rejection bandwidth. Selective (common) mode suppression can be achieved by any type of structure (not necessarily resonant elements) acting as an efficient rejection filter for the common mode and preserving signal integrity from DC up to very high frequencies for the differential mode.

COMMON-MODE REJECTION FILTERS

Common-mode rejection filters may be implemented by loading the differential lines with lumped, semi-lumped or distributed elements insensitive to differential signals, but able to prevent the propagation of the common mode. Solutions that use common-mode chokes with high permeability ferrite cores have been proposed [18-20], but chokes represent a penalty in terms of size and frequency operating range, not being useful for high-speed and high-density systems. The main focus of this article is on bi-layer structures based on symmetric patterned ground structures (PGS) [11],[16],[17],[21]-[26]. Approaches based on multilayer or LTCC technology [27]-[35] provide compact solutions, but at the expense of higher fabrication costs and complexity (especially if vias are used [28]-[30]). Common-mode filters based on periodic structures (or electromagnetic bandgaps – EBGs [36], [37]) have been also proposed [38]-[42]. Among these filters, implementations where the transverse dimensions of the differential line are periodically modulated, leaving the ground plane unaltered, have been reported [41]-[42], but at the expense of a limited common-mode rejection bandwidth.

COMMON-MODE FILTERS BASED ON PGS

Four examples of common-mode suppression filters for differential microstrip lines, based on patterned ground structures (or defected ground planes), are discussed. The ground planes of the different implementations exhibit specific patterns that efficiently suppress the common-mode, leaving the differential-mode unaltered (or almost unaltered).

Dumbbell-shaped PGS

Slotted dumbbell resonators symmetrically etched in the ground plane of a microstrip line can be modeled, to a first order approximation, as series-connected parallel resonators [43]. These resonators are thus able to inhibit signal propagation in the vicinity of resonance. The symmetry plane of the line and resonator are magnetic walls,

and this gives another interpretation to the stop band functionality of these lines, according to the symmetry considerations discussed before.

By symmetrically etching slotted dumbbell-shaped resonators in a differential microstrip line, it is expected that the common-mode will be efficiently suppressed, while signal propagation for the differential-mode is preserved. Besides the previous explanation for selective mode suppression, based on symmetry considerations, it can also be argued that the resonant elements open the return current path through the ground plane for the common-mode, whereas the presence of resonators has negligible effect on the differential signals since a relatively small current density returns through the ground plane for such signals [16]. Regardless of the specific interpretation for selective common-mode suppression in differential lines loaded with slotted dumbbell resonators, such structures behave as efficient common-mode filters. Figure 2 depicts a specific common-mode filter topology and the frequency response [16]. The structure is able to efficiently suppress the common-mode with broad stopband in the GHz range (Fig. 2b), yet keeping good differential signal integrity. In addition, mode conversion from differential-mode to common-mode, also shown in the figure, is very small.

In [16], the common-mode noise suppression capability of these dumbbell-shaped PGS structures was demonstrated in the time-domain by adding a delay line in one of the differential lines (see inset of Fig. 3). This delay line generates a signal skew which in turn excites the common mode in the differential line. By fabricating an identical structure with solid ground plane (reference board), the time domain responses to a differential signal can be compared. Two pulse trains of 800 mV peak-to-peak voltage and 8 Gb/s were differentially launched into port 1 and port 2 by the authors of [16], and the output waveforms were measured at port 3 and port 4 using a digital oscilloscope. The common-mode noise, V_{common}, defined as half of the sum of the measured voltage at these two output ports, revealed that the peak-to-peak output common-mode voltage for the reference board was 412 mV, whereas it was reduced to 64 mV by employing the dumbbell-shaped resonators (i.e., over 80% improvement was achieved), see Fig. 3. Thus, the common-mode filter based on these PGS structures is revealed to be efficient in rejecting the common mode while preserving the integrity of the differential signals. Measured differential eye diagrams not shown here, but depicted in [16], indicate that the eye diagram parameters are roughly the same in the structure of Fig. 2 and in the same structure with solid ground plane (indicating that the differential signal quality is not degraded when the common-mode filter is present).

Complementary split ring resonator (CSRR)

CSRRs, originally proposed for the implementation of epsilon-negative [12] or left-handed [44] one-dimensional metamaterials [15,45], are useful resonators for the selective suppression of the common-mode in differential microstrip lines, as anticipated before. The first common-mode filters based on CSRRs were reported in [22],[23], where it was argued that for the differential-mode there is not a net axial electric field in the inner metallic region of the CSRR able to excite the resonators,

whereas for the common-mode the electric field below the transmission lines is co-directional, and the CSRRs are excited (Fig. 4).

In order to obtain a significant common-mode rejection bandwidth, several tightly coupled resonant elements are necessary. Moreover, it is necessary to enhance the coupling capacitance between the pair of lines and the CSRRs and to reduce the inductance and capacitance of the CSRR as much as possible. This enhances the stopband bandwidth of an individual resonator, providing a wide stop band for the common mode when several tightly coupled CSRRs are considered. As reported in [22],[23], the requirements to achieve small CSRR inductance and capacitance are wide slot-ring widths and separation. To enhance the coupling capacitance between the pair of lines and the CSRR, the lines must be as wide as possible, and hence as uncoupled as possible. Note that for a given differential-mode characteristic impedance, the width of the pair of lines increases with their separation. Finally, by closely spacing the CSRRs, and by using square-shaped or rectangular CSRR geometries, inter-resonator coupling is favored.

The description of CSRR-loaded differential microstrip lines by means of a lumped element equivalent circuit model is very convenient for design purposes. However, CSRRs with wide slot-ring widths and separation cannot be considered to be electrically small. Nevertheless, by considering CSRRs with double slits (i.e., the so-called double-slit complementary split ring resonator – DS-CSRR, see the topology in Fig. 5), it is possible to obtain small inductance and capacitance with small values of ring width and separation [46]. In [23], a design procedure for such DS-CSRR based common-mode filters is reported. The design procedure is based on the lumped element equivalent circuit of the unit cell, depicted in Fig. 6 (a), where L and C are the inductance and capacitance of the lines, respectively, the resonant element (CSRR or DS-CSRR) is described by the resonant tank L_c-C_c, the coupling capacitance between resonant elements is given by C_R, and L_m and C_m account for the magnetic and electric coupling, respectively, between the pair of lines. The lumped element equivalent circuit model for the common and differential modes are depicted in Fig. 6 (b) and (c), respectively. For the differential-mode, the resulting circuit model is simply the circuit model of an ordinary line with modified parameters. The circuit model for the common mode is formally identical to that of CSRR-loaded single-ended microstrip lines with inter-resonator coupling [47], providing a stopband functionality. Using this model and the dispersion relation derived from it (inferred by means of Bloch-Floquet analysis of the multiport structure), the common-mode stopband bandwidth can be estimated [23]. Interestingly, it was demonstrated in [23] that bandwidth enhancement by inter-resonator coupling is related to the presence of complex modes [48]-[51].

Fig. 7(a) depicts a fabricated differential line loaded with symmetrically etched, rectangular-shaped and tightly coupled DS-CSRRs. The differential-mode and common-mode responses, depicted in Figs. 7(b) and (c), respectively, reveal that DS-CSRRs are efficient elements to suppress the common-mode over a wide band whilst the differential-mode is transmitted in that band (other common-mode filters based on

CSRRs are reported in [22]). Figure 8 shows the measured differential eye diagrams with the excitation of 0.2 V amplitude in 2.5 Gb/s for the differential line of Fig. 7(a) with and without DS-CSRRs. The eye diagram quality in terms of eye height, eye width, jitter and eye opening factor is very similar [23]. Therefore, the presence of the DS-CSRRs does not significantly degrade the differential signals.

Defected ground plane artificial line

Common-mode filters conceptually similar to those presented before, but implemented by means of a completely different ground plane pattern, are discussed in this section. These filters, first presented in [52] and studied in depth in [24], exhibit the topology depicted in Fig. 9. The pair of coupled microstrip lines is loaded with a periodic distribution of centered conductor patches connected to the ground plane by means of narrow (high impedance) strip lines. These lines behave as inductors in the frequency range of interest.

Under common-mode operation, the pattern printed in the ground plane, in conjunction with the coupled lines of the top side, behaves as a low-pass filter. The common-mode signal is then expected to be strongly rejected over a wide frequency band above a certain adjustable frequency. To gain insight on this, let us consider the equivalent circuit of the structure (unit cell), depicted in Fig. 10(a). In this circuit, L_s is the inductance of the lines, C_p is the capacitance between each individual line and the central patches, L_p is the inductance of the narrow strips, and C_s is the capacitance between adjacent patches. The equivalent circuits for the common and differential modes are depicted in Figs. 10(b) and (c), respectively. For the differential mode, the lumped element equivalent circuit is the one of an all-pass structure (similar to the circuit model of the CSRR, or DS-CSRR, loaded differential lines for the differential mode). Conversely, for the common-mode, the equivalent circuit indicates that signal is inhibited in certain frequency bands. If the distance between adjacent patches is significant, the coupling capacitance C_s can be neglected, and transmission zeros at the frequencies of the resulting shunt-connected series resonators (C_p-L_p) can be expected (note that if C_s is neglected, the resulting two-port of the unit cell is the building block of elliptic low-pass filters). The analysis is not so simple if such capacitances cannot be neglected. However, the resulting multiport network (common mode) can be studied by using a Bloch-Floquet analysis similar to the one applied to CSRR-based differential lines [23]. Note that the equivalent circuit of Fig. 10(b) resembles the circuit of Fig. 6(b) that describes the CSRR, or DS-CSRR, loaded differential lines for the common mode. However, the inductance L_p in the circuit of Fig. 10(b) replaces the resonant tank L_c-C_c in the circuit of Fig. 6(b). This fact is useful for achieving broader rejection bandwidths for the common mode.

A prototype device is depicted in Fig. 11(a), whereas the differential and common mode mode responses are shown in Fig. 11(b) and (c), respectively. The common-mode insertion loss is above 20 dB in the frequency range 2-4 GHz. In terms of fractional bandwidth, this result is better than those corresponding to the common-mode filters of

the previous subsections. However the maximum common-mode rejection ratio (CMRR), defined as the maximum ratio (in dB) between the transmission coefficients for the differential and common modes in the common-mode stopband region, is worse in the filter with rectangular patches and inductive strips. The presence of patches and meandered lines in the ground plane does not significantly affect the signal integrity for the differential mode, as revealed by the eye diagram compared to the one of the structure with solid ground plane (reported in [24]).

C-shaped PGS

The common-mode filters presented in this subsection (reported in [17]) are also based on patterned ground planes, but they are described by a combination of distributed and lumped components. The configuration, shown in Fig. 12, consists of a C-shaped patterned ground structure and two meandered signal lines. The C-shaped slot comprises two main components, i.e., the patch and the bridge (see Fig. 12a). The patch can be considered to be a floating ground connected to the ground plane by means of the bridge. The differential pair is composed of two meandered microstrip lines located on top of the patch, and their coupling is very weak, provided they are distant enough. Note that the C-shaped slot is a folded slotted step impedance resonator. Such a resonant element, similar to dumbbell-shaped PGS or CSRRs, exhibits a magnetic wall at its symmetry plane at the fundamental resonance. Thus, these resonant elements can be used for the suppression of the common mode following a methodology analogous to the one for CSRRs or dumbbell-shaped PGS based common-mode filters. However, in the configuration of Fig. 12, the C-shaped slot cannot be considered to be electrically small at the frequencies of interest, and therefore, a mixed distributed-lumped analysis is required.

The circuit schematic of the structure of Fig. 12 is depicted in Fig. 13(a). The patch and the meandered lines on top of it are modeled as a coupled transmission line with single-ended characteristic impedance Z_1 and corresponding electrical length θ_1. The C-shaped slot can be considered as four slot-lines: two of them with impedance and electrical length Z_2 and θ_2, respectively, and the other two with impedance and electrical length Z_3 and θ_3, respectively. Note that the two different slot-lines are connected in series and shunt between the patch and ground plane, as shown in Fig. 13(a). The bridge is described by a partial inductance L_b. Similarly, the signal line sections on top of the bridge are also modeled as partial inductances L_s due to the lack of ground metallization below them. The mutual inductances between the signal lines and between the signal line and bridge are also considered in [17]. Such mutual inductances are denoted as L_{ss} and L_{sb}.

The circuit models under differential and common mode excitation are depicted in Figs. 13(b) and (c), respectively, with the indicated equivalence between inductive elements. For the differential mode, the structure is all-pass, according to the circuit model. Conversely, the common-mode is rejected in a certain frequency band due to the interaction of the signal lines, slot lines, and the bridge. Note that this rejection

mechanism is different than those of the previous common-mode stopband filters, where the common mode is rejected by a resonance-associated phenomenon.

The analysis of the circuit of Fig. 13(c), detailed in [17], gives an expression providing the position of the transmission zero frequencies. Based on this formula, a systematic synthesis method for common-mode stop band filters based on these C-shaped slot structures, with transmission zeros for that mode at desired frequencies, is detailed in [17].

An example of a common-mode stopband filter, with transmission zeros located at 2.6 GHz and 6.6 GHz is depicted in Fig. 14(a), and the corresponding frequency response (common-mode and differential-mode insertion loss) is depicted in Fig. 14(b). It is remarkable that the filter is transparent for the differential mode, with differential mode insertion loss lower than 3 dB from DC up to 9 GHz. However, for the common mode, a −10 dB fractional bandwidth of 130% is obtained, thanks to the two transmission zeros for that mode. The dimensions are as small as 5.6×5.65 mm^2 (i.e., 0.04 λ^2, where λ is the wavelength of the stopband central frequency).

COMMON-MODE FILTERS BASED ON PERIODIC STRUCTURES

Periodic structures are able to inhibit signal propagation at certain frequencies due to the well-known Bragg effect, derived from periodicity [36],[37]. In microwave engineering, periodic transmission lines are usually referred to as electromagnetic bandgap (EBG) based lines, analogous to photonic bandgaps, that is, periodic structures operating at optical frequencies (also known as photonic crystals). Periodicity can be achieved by etching patterns in the ground plane [53],[54], by modulating the transverse dimensions of the line (non-uniform transmission lines) [55],[56] or by periodically loading the line with reactive elements [57],[58]. Microstrip reflectors implemented by periodic non-uniform transmission lines with line width modulation have been reported [56]. According to the Bragg condition, the first forbidden band appears in the vicinity of the frequency satisfying that the period is half the guided wavelength (further band gaps may appear at harmonic frequencies, depending on the harmonic content of the periodic function describing the periodicity) [1],[36],[37]. The bandwidth and rejection level are determined by the number of stages and by the magnitude of the modulation, according to formulas inferred from the coupled mode theory [1],[59],[60].

The reflection properties of EBGs can be used for the selective mode suppression of the common mode in differential microstrip lines. The principle is as simple as determining the transverse dimensions of the line (as a function of the position along it) that are necessary to leave the differential-mode impedance unaltered and, at the same time, periodically modulate the common-mode impedance with a half wavelength period. Under these conditions, the differential line “emulates” a uniform line for the differential mode and a Bragg reflector for the common-mode. One key advantage of this approach is that the ground plane is kept unaltered. However, bandwidth is limited since, given a minimum rejection level at the Bragg frequency (where maximum

attenuation occurs), bandwidth is dictated by the magnitude of the modulation [1],[60] and it is limited in practice by the critical (minimum) dimensions (slot and line width) of the technology in use. Common-mode rejection bandwidth can be expanded by cascading several periodic EBG structures with different periods [41], or by means of chirping techniques [42]. Figure 15(a) depicts a common-mode suppressed differential line designed by considering two cascaded periodic structures with periods l_1= 2.85 cm and l_2= 2.04 cm, corresponding to Bragg frequencies of f_{B1} = 2 GHz and f_{B2} = 2.8 GHz, respectively, in the considered substrate. The specific dependence of the common-mode impedance with the position along the line for each EBG was calculated in [41], in order to obtain maximum attenuation of 13 dB with a bandwidth of 66% (f_{B1}) and 93.6% (f_{B2}), considering 3 cells. The previous attenuations and bandwidths correspond to the individual structures. By cascading them, a broader common-mode rejection bandwidth in the vicinity of 2.4 GHz results. Figs. 15(b) and (c) illustrate the insertion and return losses for the common and differential modes. The common-mode insertion loss of a single-tuned EBG-based line with 6 periods and comparable rejection level (30 dB) at 2.4 GHz is also included for comparison purposes. The bandwidth can be notably improved by using two cascaded EBGs, without a penalty in device size (both are comparable). Common-mode suppression filters based on chirped EBGs can be found in [42].

Another approach for the implementation of common-mode suppressed differential lines based on EBGs utilizes the so-called uniplanar compact photonic-bandgap (UC-PBG) ground plane concept [61]. These common-mode filters, first presented in [40], exhibit wide stopband bandwidths for the common mode, but at the expense of etching the ground plane. The UC-PBG is a two dimensional array of complementary Jerusalem crosses that behave as parallel LC tanks, thus presenting a high impedance path for the currents traveling through the structure. The capacitance and inductance are provided by the thin gap between the adjacent metallic patches and the narrow branches connecting each unit-cell, respectively. This structure exhibits a significant slow-wave effect [61] that substantially increases the phase constant in the propagation bands. The result is that compact EBG stop band structures can be achieved with this approach. The structure reported in [40], where 10 unit cells are etched in the ground plane, is depicted in Fig. 16(a), whereas the frequency response is shown in 16(b). The design procedure was based on the dispersion analysis, using eigenmode solvers. The differential mode signals are insensitive to the presence of the UC-PBG structure up to roughly 8.5 GHz, whereas the common mode is rejected with a suppression level below −20 dB between 3.3 GHz and 7 GHz, representing a fractional bandwidth of 70%.

Other EBG-based common mode stop band filters that use three metal levels have been presented in [38],[39], but these filters are able to suppress specific frequencies, as compared to the realizations presented so far.

OTHER COMMON-MODE FILTERS

In the previous approaches, common mode suppression was achieved by considering planar structures with only two metal levels. In this section, other common-mode stop band filters based on multilayer structures are presented. In [28],[34] the structures consist of a pair of differential lines (top metallic layer) on top of metallic patches (central layer) connected to the ground (third layer) through metallic vias. The circuit model of the unit cell is identical to the one depicted in Fig. 6(a), describing the unit cell of the CSRR- or DS-CSRR-based common-mode stop band filters discussed before. Thus, the common mode suppression principle is identical to the one detailed before in reference to CSRR and DS-CSRR common mode filters. Ground plane etching is not required, but three metal levels are needed.

In [30], the authors present a common mode stop band filter that also uses three metal layers. The differential pair strips are etched in the top layer, whereas in the central layer a quarter wavelength open stub, connected to the ground plane (third layer) through a metallic via, is defined and located beneath the differential lines. For differential mode excitation, the symmetry plane is an electric wall, and the effects of the open stub are cancelled; therefore, the structure is transparent for that mode. However, for the common mode, the pair of lines is efficiently coupled to the open stub, resulting in a stopband for that mode in the vicinity of the design frequency (the one giving a quarter wavelength stub). By cascading three unit cells, it is demonstrated in [30] that a stop band bandwidth from 3.7 GHz to 7.3 GHz with common mode rejection better than 20 dB can be achieved, preserving good signal integrity for the differential signals.

The solution proposed in [29] is conceptually similar to the one proposed in [17] (C-shaped PGS). In [31], common-mode filters based on CSRRs similar to those discussed before (and reported in [22],[23]), are presented. The common-mode filters of [25] are indeed those reported in [16], based on dumbbell shaped PGSs. However, to reduce size and improve the quality of the differential signals, a slow wave structure and open stubs are added to the differential lines. The filters reported in [26] are also conceptually similar to those of [16], but utilize the mutual inductance and capacitance between DGS patterns to improve the common-mode rejection bandwidth. This mutual coupling between resonant patterns is also exploited in [21].

One of the formerly proposed common mode stopband filters, implemented in multilayer low temperature co-fired ceramic (LTCC) technology [27], exhibits reasonable performance, but at the expense of a complex fabrication process and design methodology. This also applies to a recently reported type of common-mode filter [33], based on modified T-circuits and implemented in multilayer integrated passive device (IPD) processes. Nevertheless, these later common-mode stop band filters exhibit a very wide stopband for the common mode (with a differential band extending up to roughly 10GHz) and are extremely small, as compared to any other implementation.

CONCLUSIONS

In this article, recently proposed common-mode stopband filters for balanced transmission lines based on various approaches, all of them exploiting symmetry properties, have been discussed. Particular emphasis has been given to two-layer (metallic) structures, including common-mode filters based on dumbbell shaped PGSs, CSRRs, defected ground plane artificial lines and C-shaped PGS, as well as common-mode filters implemented by means of EBGs. Other common-mode filters based on multilayer, LTCC or IPD technologies have been also (briefly) discussed, or properly referenced. In general with these later technologies, further size reduction can be achieved, but at the expense of higher fabrication complexity. A comparison between the different common-mode filters, in terms of number of layers, size, fractional bandwidth (for the common mode) and common-mode rejection ratio (CMRR), is presented in Table I.

Table I: Comparison of several common-mode stopband filters based on different techniques

Reference	*Layers*	*Area* ($\lambda\times\lambda$)	−10 dB *FBW* (%)	*CMRR* (dB)
[16]	2	0.76×0.47	70	>35
[22]	2	0.43×0.14	54	>30
[23]	2	0.64×0.13	51	>40
[24]	2	0.32×0.22	100	>20
[17]	2	0.20×0.20	130	>12
[41]*	2	3.14×0.19	67	>25
[42]*	2	6.20×0.28	80	>30
[40]	2	-------	83	>40
[28]	3	0.26×0.16	60	>40
[30]	3	-------	73	>35
[29]	4	0.12×0.12	104	>10
[25]	2	-------	95	>25
[27]	LTCC	-------	150	>25
[21]	2	0.44×0.44	87	>15
[33]	3	0.017×0.016	100	>12
[34]	3	0.43×0.19	27	>25
[26]	2	--------	140	>25

*Note that these filters use two metal layers, the bottom one being a solid ground plane and hence not an active layer.

By reviewing the information in the table, there is not an optimum implementation. In general very small size is achieved by using multilayer or LTCC technology, as expected, but the CMRR in these common-mode filters is not very high, with the exception of the filter proposed in [28], where a CMRR above 40 dB was achieved. However, in this filter the −10 dB common-mode fractional bandwidth is small as

compared to those of the filters of references [27],[29],[30],[33]. In terms of CMRR, besides the filter in [28], the best filters are those of references [23], [40]. These filters use two metal layers, but the filter in [40] occupies significant area, as compared to the filter in [23]. The common-mode filters reported in [17],[24] exhibit significant bandwidth and relatively small size, and are good solutions in applications where only two metal layers are allowed or fabrication complexity must be minimized (however, the CMRR in the filter of [17] is very limited). Two-layer common-mode filters such as those reported in [23],[24] have been applied to the enhancement of common-mode suppression in planar balanced filters, also reported in [23],[24]. For this particular application, small size and implementation in PCB technology are key aspects. Nevertheless, an intensive research activity on balanced microwave filters with inherent common-mode suppression has been carried out in the last years (see [62] and references therein for wideband balanced filters, and the book [63] –to be published soon– devoted to balanced microwave filters).

ACKNOWLEDGMENTS

The authors are grateful for the support of MINECO, Spain (projects TEC2013-40600-R and TEC2013-41913-P), Generalitat de Catalunya (project 2014SGR-157), Institució Catalana de Recerca i Estudis Avançats (who awarded Ferran Martín), and FEDER.

References

1. F. Martín, *Artificial Transmission Lines for RF and Microwave Applications*, John Wiley, Hoboken, NJ, 2015.
2. J. Naqui, *Symmetry properties in Transmision Lines Loaded with Electrically Small Resonators: Circuit Modeling and Applications*, Springer, Heidelberg, Germany, 2016.
3. J. Naqui, M. Durán-Sindreu and F. Martín, "Novel sensors based on the symmetry properties of split ring resonators (SRRs)", *Sensors*, vol 11, pp. 7545-7553, 2011.
4. J. Naqui, M. Durán-Sindreu, and F. Martín, "Alignment and position sensors based on split ring resonators", *Sensors*, vol. 12, pp. 11790-11797, 2012.
5. J. Naqui, and F. Martín, "Transmission lines loaded with bisymmetric resonators and their application to angular displacement and velocity sensors", *IEEE Trans. Microw. Theory Techn.*, vol. 61(12), pp. 4700-4713, Dec. 2013.
6. A. Karami-Horestani, C. Fumeaux, S.F. Al-Sarawi, and D. Abbott, "Displacement sensor based on diamond-shaped tapered split ring resonator", *IEEE Sensors J*., vol. 13, pp. 1153-1160, 2013.
7. J. Naqui, and F. Martín, "Angular displacement and velocity sensors based on electric-LC (ELC) loaded microstrip lines", *IEEE Sensors J.*, vol. 14(4), pp. 939-940, Apr. 2014.
8. A.K. Horestani, J. Naqui, D. Abbott, C. Fumeaux, and F. Martín, "Two-dimensional displacement and alignment sensor based on reflection coefficients of open microstrip lines loaded with split ring resonators", *Electronics Letters*, vol. 50, pp. 620-622, Apr. 2014.
9. J. Naqui, M. Durán-Sindreu, F. Martín, "Selective mode suppression in coplanar waveguides using metamaterial resonators", *Appl. Phys. A - Materials Science and Processing*, vol. 109, pp. 1053-1058, Dec. 2012.
10. J. Naqui, M. Durán-Sindreu, F. Martín, "Differential and single-ended microstrip lines loaded with slotted magnetic-LC (MLC) resonators", *Int. J. Ant. Propag.*, article ID 640514, 8 pages, 2013.
11. J. Naqui, M. Durán-Sindreu, and F. Martín, "Selective mode suppression in microstrip differential lines by means of electric-LC (ELC) and magnetic-LC (MLC) resonators", *Appl. Phys A*, vol. 115, pp. 637-643, 2014.
12. F. Falcone, T. Lopetegi, J.D. Baena, R. Marqués, F. Martín and M. Sorolla, "Effective negative-epsilon stop-band microstrip lines based on complementary split ring resonators", *IEEE Microw. Wireless Compon. Lett.*, vol. 14, pp. 280-282, June 2004.

13. J.B. Pendry, A.J. Holden, D.J. Robbins and W.J. Stewart, “Magnetism from conductors and enhanced nonlinear phenomena”, *IEEE Transactions Microwave Theory Tech.*, vol. 47, pp. 2075-2084, Nov. 1999.
14. R. Marqués, F. Medina and R. Rafii-El-Idrissi, “Role of bianisotropy in negative permeability and left handed metamaterials”, *Phys. Rev. B*, vol. 65, pp. 144441 (1-6), 2002.
15. R. Marqués, F. Martín and M. Sorolla, *Metamaterials with negative parameters: theory, design and microwave applications*, John Wiley, Hoboken, NJ, 2008.
16. W. T. Liu, C.-H. Tsai, T.-W. Han and T.-L. Wu, “An embedded common-mode suppression filter for GHz differential signals using periodic defected ground plane,” *IEEE Microw. Wireless Compon. Lett.*, vol. 18, no. 4, pp. 248–250, Apr. 2008.
17. T.W. Weng, C.H. Tsai, C.H. Chen, D.H. Han and T.L. Wu, “Synthesis model and design of a common-mode bandstop filter (CM-BSF) with an all-pass characteristic for high-speed differential signals”, *IEEE Trans. Microw. Theory Techn*., vol. 62, no. 8, pp. 1647-1656, Aug. 2014.
18. J. D. Gavenda, “Measured effectiveness of a toroid choke in reducing common-mode current,” in *Proc. IEEE Int. Electromagn. Compat. Symp*., 1989, pp. 208-210.
19. K. Yanagisawa, F. Zhang, T. Sato, and Y. Miura, “A new wideband common-mode noise filter consisting of Mn–Zn ferrite core and copper/polyimide tape wound coil,” *IEEE Trans. Magn*., vol. 41, no.10, pp. 3571-3573, Oct. 2005.
20. J. Deng and K. Y. See, “In-circuit characterization of common-mode chokes”, *IEEE Trans. Electromagn. Compat*., vol. 49, no. 5, pp. 451-454, May 2007.
21. S. J. Wu, C. H. Tsai, T. L. Wu, and T. Itoh, “A novel wideband common-mode suppression filter for gigahertz differential signals using coupled patterned ground structure”, *IEEE Trans. Microw. Theory Techn*., vol. 57, no. 4, pp. 848–855, Apr. 2009.
22. J. Naqui, A. Fernández-Prieto, M. Durán-Sindreu, J. Selga, F. Medina, F. Mesa, and F. Martín, “Split rings-based differential transmission lines with common-mode suppression”, *IEEE MTT-S Int. Microwave Symposium*, Baltimore (USA), June 2011.
23. J. Naqui, A. Fernández-Prieto, M. Durán-Sindreu, F. Mesa, J. Martel, F. Medina, and F. Martín, “Common mode suppression in microstrip differential lines by means of complementary split ring resonators: theory and applications”, *IEEE Trans. Microw. Theory Techn*., vol. 60, pp. 3023-3034, Oct. 2012.
24. A. Fernandez-Prieto, J. Martel-Villagrán, F. Medina, F. Mesa, S. Qian, J-.S Hong, J. Naqui, F. Martin, “Dual-band differential filter using broadband common-mode rejection artificial transmission line”, *Prog. Electromagn. Research* (PIER), vol. 139, pp. 779-797, 2013.
25. F.X. Yang, M. Tang, L.S. Wu, and J.F. Mao, “A novel wideband common-mode suppression filter for differential signal transmission”, *2014 IEEE Electrical Design of Advanced Packaging & Systems Symposium* (EDAPS), Bangalore, Dec. 2014, pp. 129-132.
26. Z. Zeng, Y. Yao, and Y. Zhuang, “A wideband common-mode suppression filter with compact-defected ground structure pattern”, *IEEE Trans. Electromagn. Compt*., vol. 57, pp. 1277-1280, Oct. 2015
27. B. C. Tseng and L. K. Wu, “Design of miniaturized common-mode filter by multilayer low-temperature co-fired ceramic”, *IEEE Trans. Electromagn. Compat.*, vol. 46, no. 4, pp. 571–579, Nov. 2004.
28. C.-H. Tsai and T.-L. Wu, “A broadband and miniaturized common mode filter for gigahertz differential signals based on negative-permittivity metamaterials,” *IEEE Trans. Microw. Theory Tech*., vol. 58, no. 1, pp. 195–202, Jan. 2010.
29. C. Y. Hsiao, C. H. Tsai, C. N. Chiu, and T. L. Wu, “Radiation suppression for cable-attached packages utilizing a compact embedded common-mode filter”, *IEEE Trans. Compon. Packag., Manuf. Technol.*, vol. 2, no. 10, pp. 1696–1703, Oct. 2012.
30. G.H. Shiue, C.M. Hsu, C.L. Yeh and C.F. Hsu, “A comprehensive investigation of a common-mode filter for gigahertz differential signals using quarter-wavelength resonators”, *IEEE Trans. Compon. Packag., Manuf. Technol.*, vol. 4, no. 1, pp. 134-144, Jan. 2014.
31. S.G. Kang, G. Shaffer, C. Kodama, C. O’Daniel and E. Wheeler, “CSRR common-mode filtering structures in multilayer printed circuit boards”, *2015 IEEE International Symposium on Electromagnetic Compatibility* (EMC 2015), Dresden, Germany, Aug. 2015, pp. 1300-1303.
32. C.H. Cheng and T.L. Wu, “A compact dual-band common-mode filtering component for EMC in wireless communication”, *2015 Asia-Pacific International EMC Symposium* (APEMC 2015), Taipei, Taiwan, May 2015.
33. C.Y. Hsiao, Y.C. Huang, and T.L. Wu, “An ultra-compact common-mode bandstop filter with modified-t circuits in integrated passive device (IPD) process”, *IEEE Trans. Microw. Theory Techn*., vol. 63, no 11, pp. 3624-3631, Nov. 2015.

34. A. Fernández-Prieto, S. Qian, J. Hong, J. Martel, F. Medina, F. Mesa, J. Naqui, and F. Martín "Common-mode suppression for balanced bandpass filters in multilayer liquid crystal polimer technology", *IET Microw. Ant. Propag.*, vol. 9, pp. 1249-1253, Sep. 2015.
35. B.-F. Su and T.-G. Ma, "Miniaturized common-mode filter using coupled synthetsized lines and mushroom resonators for high-speed differential signals", *IEEE Microw. Wireless Compon. Lett*., vol. 25, pp.112-114, Feb. 2015.
36. E. Yablonovitch, "Photonic band gap structures", *J. Opt. Soc. Amer. B* 10, pp. 283-295, 1993.
37. J. D. Joannopoulos, R. D. Meade, and J. N. Winn, *Photonic Crystals: Molding the Flow of Light*, Princeton, NJ, Princeton University Press, 1995.
38. F. de Paulis, L. Raimondo, Sam Connor, B. Archambeault and A, Orlandi, "Design of a common mode filter by using planar electromagnetic bandgap structures", *IEEE Trans. Adv. Packag*., vol. 33, no. 4, pp. 994-1002, Nov. 2010.
39. F. de Paulis, L. Raimondo, Sam Connor, B. Archambeault and A. Orlandi, "Compact configuration for common mode filter design based on planar electromagnetic bandgap structures", *IEEE Trans. Electromagn. Compat.*, vol. 54, no. 3, pp. 646-654, Jun. 2012.
40. J. H. Choi, P. W. C. Hon and T. Itoh, "Dispersion analysis and design of planar electromagnetic bandgap ground plane for broadband common-mode suppression", *IEEE Microw. Wireless Comp. Lett.*, vol. 24, no. 11, pp. 772-774, Nov. 2014.
41. P. Vélez, J. Bonache, and F. Martín, "Differential Microstrip Lines with Common-Mode Suppression based on Electromagnetic Bandgaps (EBGs)", *IEEE Ant. Wireless Propag. Lett.*, vol. 14, pp. 40-43, 2015.
42. P. Vélez, M. Valero, L. Su, J. Naqui, J. Mata-Contreras, J. Bonache, and F. Martín, "Enhancing common-mode suppression in microstrip differential lines by means of chirped electromagnetic bandgaps (EBGs)", *Microw. Opt. Technol. Lett.*, vol. 58, pp. 328–332, Feb. 2016.
43. D. Ahn, J.-S. Park, C.-S. Kim, J. Kim, Y. Qian, and T. Itoh, "A design of the low-pass filter using the novel microstrip defected ground structure", *IEEE Trans. Microw. Theory Tech.*, vol. 49, pp. 86-93, 2001.
44. F. Falcone, T. Lopetegi, M.A.G. Laso, J.D. Baena, J. Bonache, R. Marqués, F. Martín, M. Sorolla, "Babinet principle applied to the design of metasurfaces and metamaterials", *Phys. Rev. Lett*., vol. 93, paper 197401, Nov. 2004.
45. J.D. Baena, J. Bonache, F. Martín, R. Marqués, F. Falcone, T. Lopetegi, M.A.G. Laso, J. García, I Gil, M. Flores-Portillo and M. Sorolla, "Equivalent circuit models for split ring resonators and complementary split rings resonators coupled to planar transmission lines", *IEEE Trans. Microw. Theory Techn*., vol. 53, pp. 1451-1461, Apr. 2005.
46. R. Marqués, J.D. Baena, J. Martel, F. Medina, F. Falcone, M. Sorolla and F. Martín, "Novel small resonant electromagnetic particles for metamaterial and filter design" *Proc. Int. Conf. Electromagn. Advan. Appl.*, ICEAA, 2003, pp. 439-443, 8-12 Sep. 2003, Torino (Italy).
47. J. Naqui, M. Durán-Sindreu, A. Fernández-Prieto, F. Mesa, F. Medina, and F. Martín, "Multimode propagation and complex waves in CSRR-based transmission line metamaterials", *IEEE Ant. Wireless Propag. Lett.*, vol. 11, pp. 1024-1027, 2012.
48. F. A. Fernández, Y. Lu, J. B. Davies, and S. Zhu, "Finite element analysis of complex modes in inhomogeneous waveguides," *IEEE Trans. Magn*., vol. 29, pp. 1601–1604, Mar. 1993.
49. U. Crombach, "Complex waves on shielded lossless rectangular dielectric image guide," *Electron. Lett*., vol. 19, pp. 557-558, Jul. 1983.
50. M. Mrozowski and J. Mazur, "Matrix theory approach to complex waves," *IEEE Trans. Microw. Theory Tech.*, vol. 40, no. 4, pp. 781-785, Apr. 1992.
51. F. Elek and G. V. Eleftheriades, "Dispersion analysis of the shielded Sievenpiper structure using multiconductor transmission line theory," *IEEE Microw.Wireless Compon. Lett*., vol. 14, no. 9, pp. 434-436, Sep. 2004.
52. A. Fernández-Prieto, J. Martel, J.S. Hong, F. Medina, S. Qian, and F. Mesa, "Differential transmission line for common-mode suppression using double side MIC technology," *Proc. of the 41st European Microwave Conference* (EuMC), 631-634, Manchester, England, UK, Oct. 10-13, 2011.
53. V. Radisic, Y. Qian, R. Coccioli, T. Itoh, "Novel 2-D photonic bandgap structure for microstrip lines", *IEEE Microw. Guided Wave Lett*., vol. 8, pp. 69-71, 1998.
54. F. Falcone, T. Lopetegi, and M. Sorolla, "1-D and 2-D photonic bandgap microstrip structures", *Microw. Opt. Techn. Lett*., vol. 22, pp. 411- 412, 1999.
55. T. Lopetegi, M.A.G. Laso, F. Falcone, F. Martín, J. Bonache, L. Pérez-Cuevas, M. Sorolla, "Microstrip wiggly line band pass filters with multispurious rejection", IEEE Microwave and Wireless Components Letters, vol. 14, pp. 531-533, November 2004.

56. I. Arnedo, M. Chudzik, J. Schwartz, I. Arregui, A. Lujambio, F. Teberio, D. Benito, M.A.G. Laso, D. Plant, J. Azaña, and T. Lopetegi, “Analytical solution for the design of planar EBG structures with spurious-free frequency response”, *Microw. Opt. Techn. Lett*., vol. 54, pp. 956-960, 2012.
57. A. Görür, C. Karpuz and M. Alkan, “Characteristics of periodically loaded CPW structures”, *IEEE Microw. Guided Wave Lett.*, vol. 8, pp. 278-280, 1998.
58. F. Martín, F. Falcone, J. Bonache, T. Lopetegi, M.A.G. Laso, M. Sorolla, “New periodic-loaded electromagnetic bandgap coplanar waveguide with complete spurious passband suppression”, *IEEE Microw. Wireless Compon. Lett*., vol. 12, pp. 435-437, 2002.
59. B. Z. Katsenelenbaum, L. Mercader, M. Pereyaslavets, M. Sorolla, and M. Thumm, *Theory of Nonuniform Waveguides – the Cross-section Method*, London, UK, IEE Electromagnetic Waves Series, 44, 1998.
60. T. Lopetegi, *Photonic Band Gap Structures in Microstrip Technology: Study Using the Coupled Mode Formalism and Applications*, PhD Thesis Dissertation, Pamplona, Spain, 2002.
61. F. R. Yang, K. P.Ma, Y. Qian, and T. Itoh, “A uniplanar compact photonic-bandgap (UC-PBG) structure and its applications for microwave circuits,” *IEEE Trans. Microw. Theory. Tech*., vol. 47, pp. 1509–1514, Aug. 1999.
62. W. Feng, W. Che, and Q. Xue, “The proper balance: overview of microstrip wideband balanced circuits with wideband common mode suppression”, *IEEE Microwave Magazine*, vol. 16, pp. 55-68, June 2015.
63. F. Martín, L. Zhu, F. Medina and J.S Hong, *Balanced Microwave Filters*, John Wiley, Hoboken, NJ, to be published.

Figures

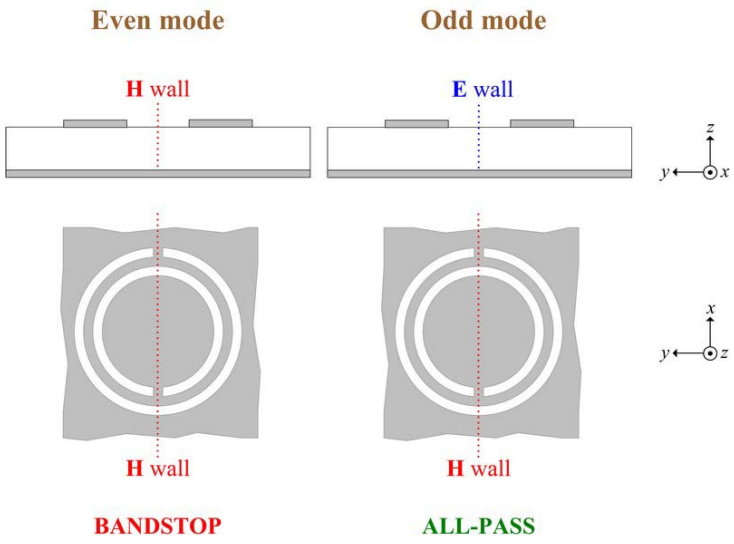

(a)

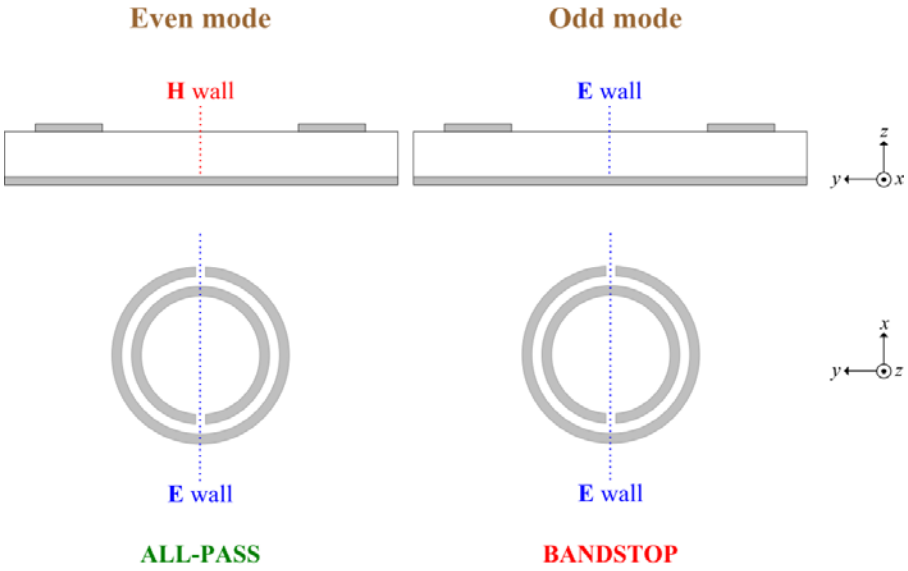

(b)

Figure 1. Illustration of selective mode suppression in microstrip differential lines by using CSRRs etched in the ground plane (a), and SRRs etched in the upper metal layer, between the pair of lines (b).

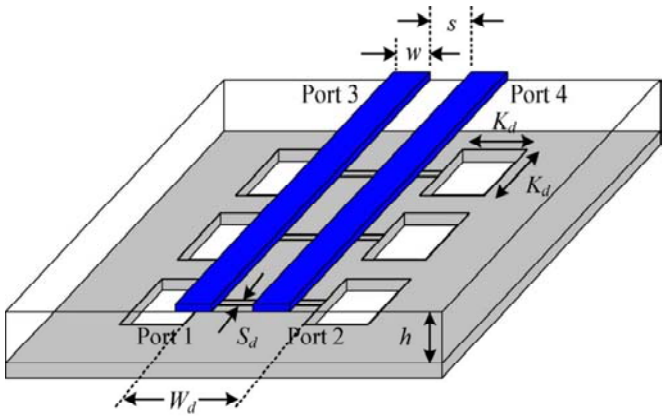

(a)

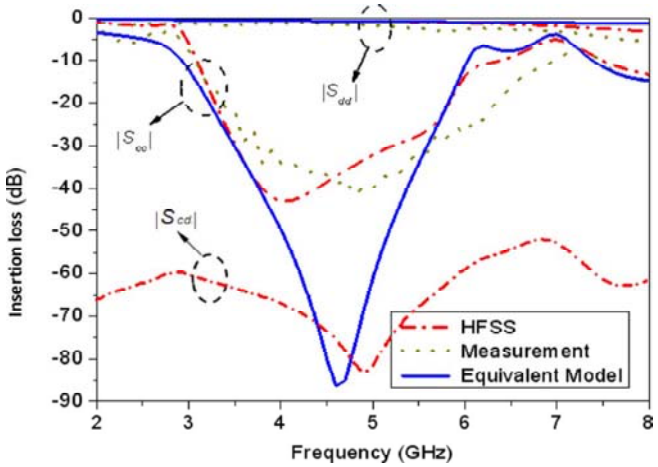

(b)

Figure 2. Common-mode stop band filter implemented by slotted dumbbell-shaped resonators (a), and frequency response for the differential (S_{dd}) and common modes (S_{cc}) (b). The simulated transmission of mode-conversion from differential mode to common mode, S_{cd}, is also shown in (b). Reprinted with permission from Ref. [16]; copyright 2008 IEEE.

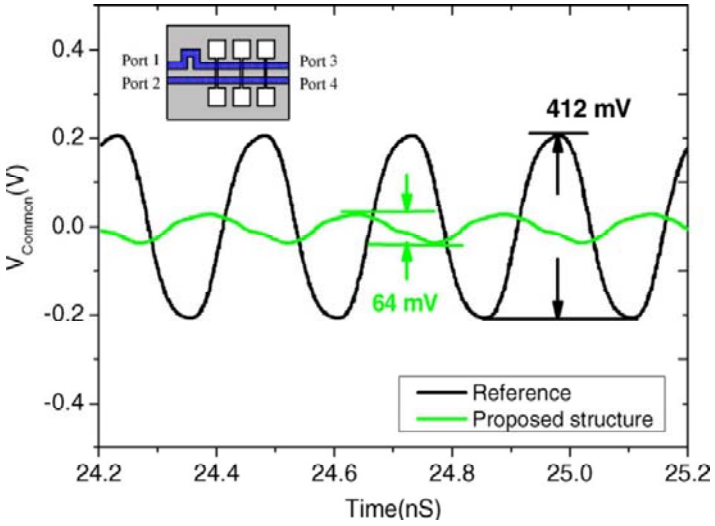

Figure 3. Measured time-domain waveforms for common-mode output of the reference differential structure (without patterned ground plane) and the proposed structure of ref. [16] (with slotted dumbbell resonators). Reprinted with permission from Ref. [16]; copyright 2008 IEEE.

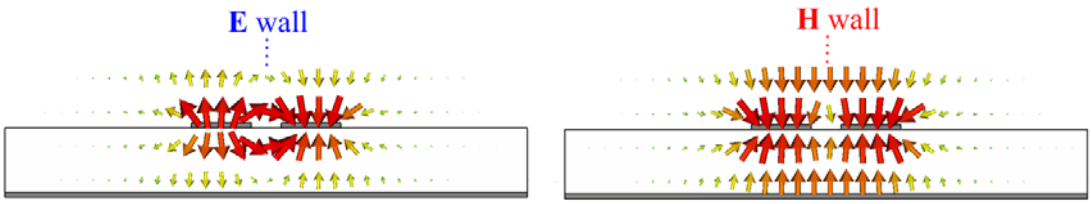

Figure 4. Cross sectional view of a differential microstrip line and electric field lines for the differential (a) and common (b) modes.

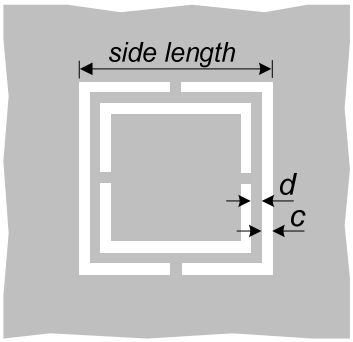

Figure 5. Topology of the square-shaped DS-CSRR

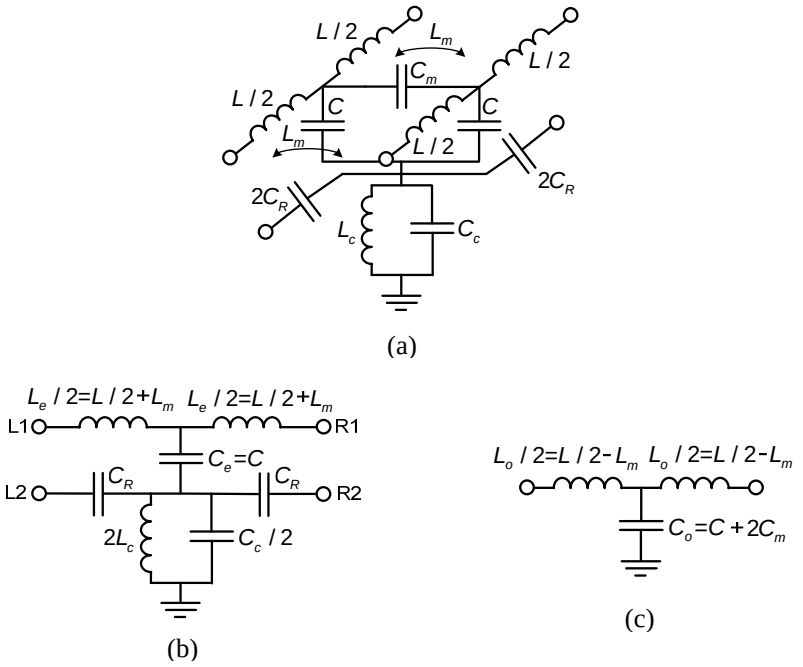

Figure 6. Lumped element equivalent circuit model (unit cell) of a differential microstrip line loaded with CSRRs or DS-CSRRs (a), equivalent circuit model for the common mode (b), and equivalent circuit model for the differential mode (c).

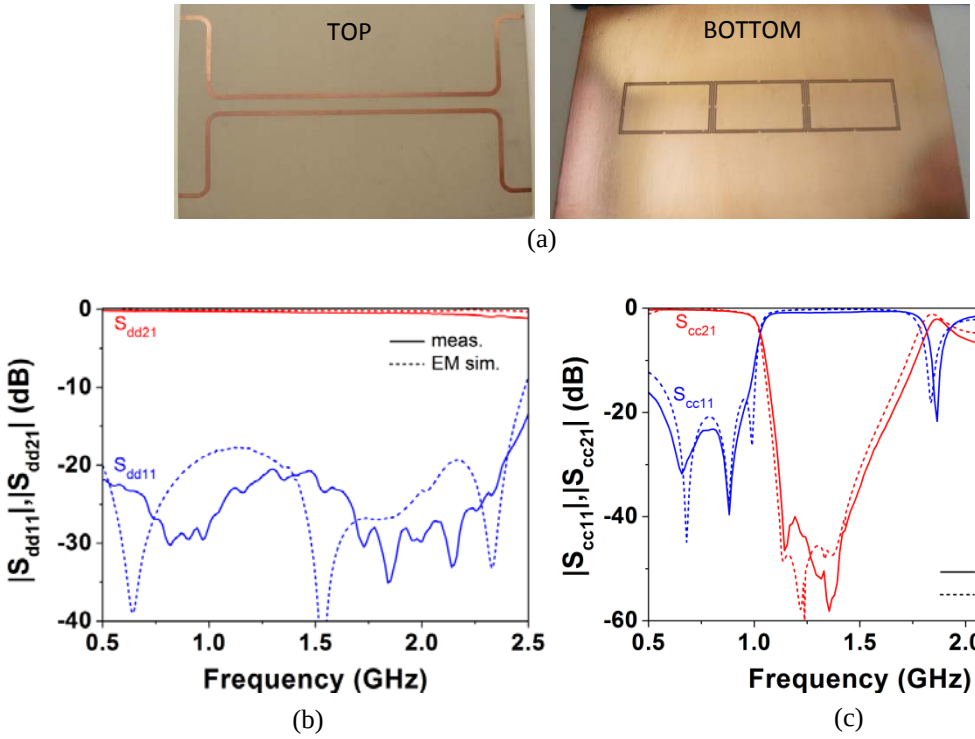

Figure 7. Photograph (a), differential-mode return loss $|S_{dd11}|$ and insertion loss $|S_{dd21}|$ (b), and common-mode return loss $|S_{cc11}|$ and insertion loss $|S_{cc21}|$ (c) of the differential line with common-mode suppression based on DS-CSRRs. Reprinted with permission from [23]; copyright 2012 IEEE.

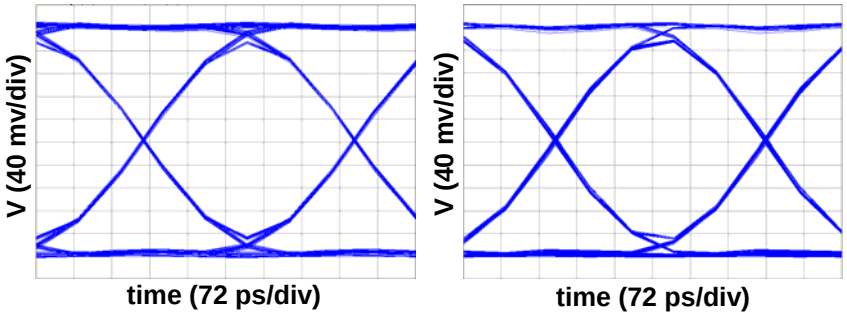

(a) (b)

Figure 8. Measured differential eye diagrams for the differential line of Fig. 7 with (a) and without (b) DS-CSRRs. Reprinted with permission from [23]; copyright 2012 IEEE.

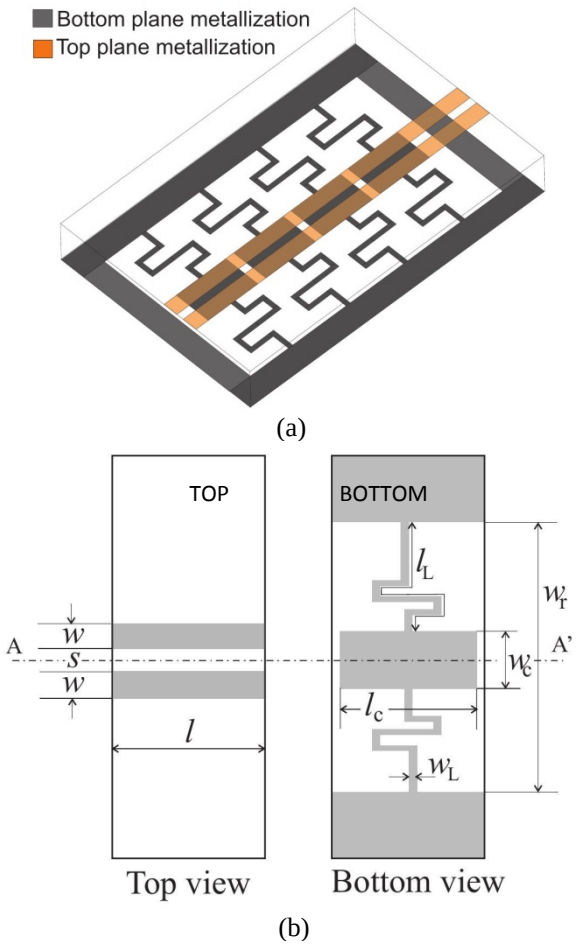

Figure 9. 3D view (a) and layout (unit cell) (b) of the common-mode suppression filter based on rectangular patches connected to the ground plane through meandered inductive strips. The metallic regions in (b) are indicated in gray.

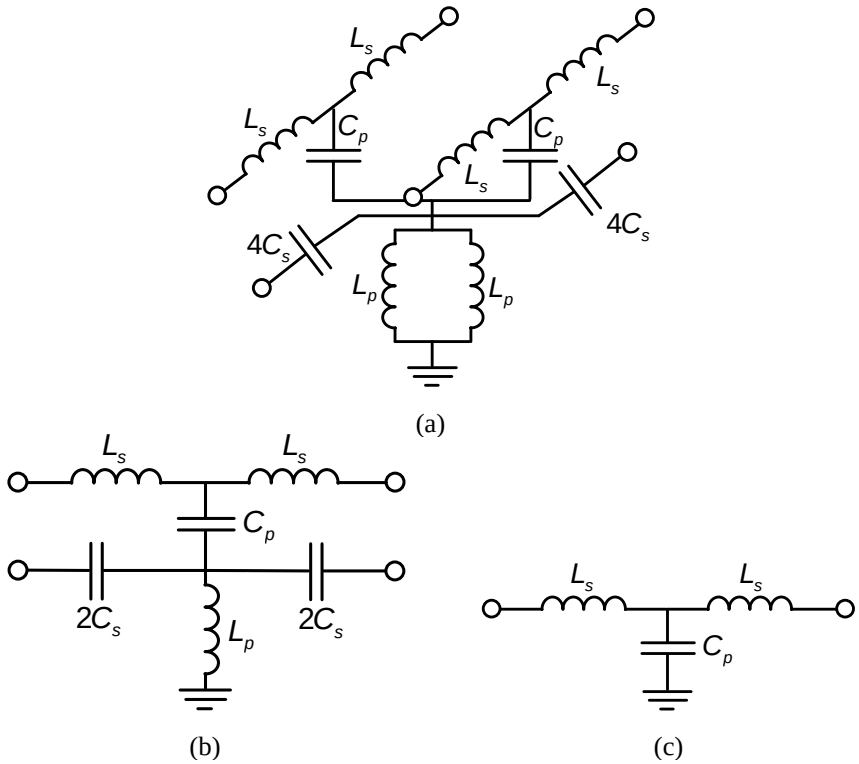

Figure 10. Lumped element equivalent circuit model (unit cell) of a differential microstrip line loaded with rectangular patches connected to the ground plane by inductive strips (a), equivalent circuit model for the common mode (b), and equivalent circuit model for the differential mode (c). The nomenclature used for the different elements is the one of [24], different than the one used in Fig. 6.

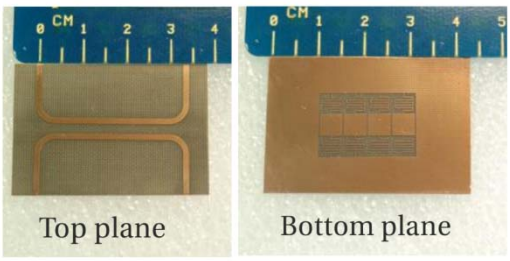

(a)

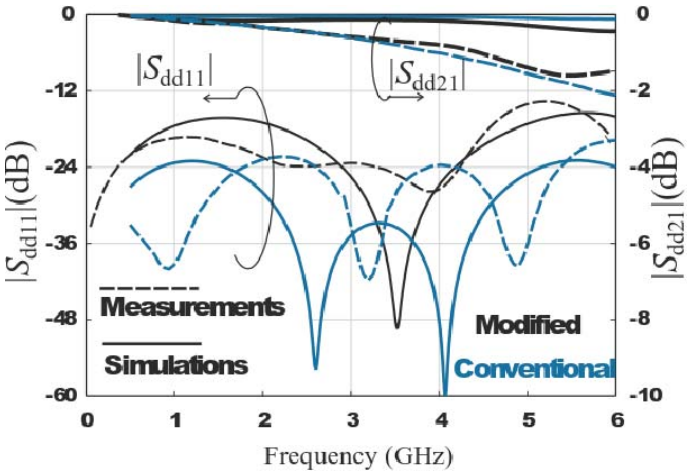

(b)

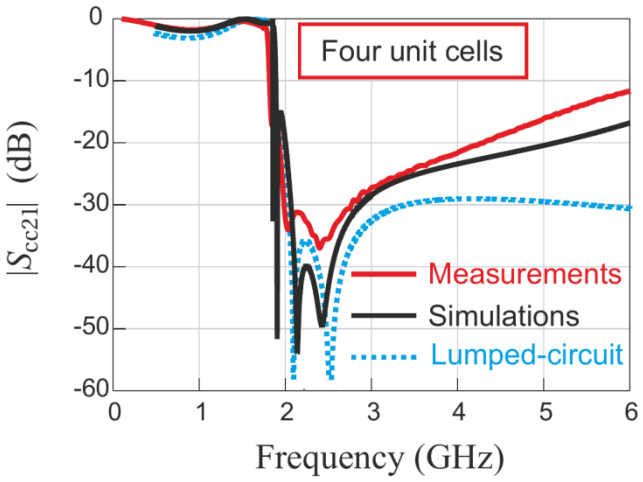

(c)

Figure 11. Photograph (a), differential-mode return loss $|S_{dd11}|$ and insertion loss $|S_{dd21}|$ (b), and common-mode insertion loss $|S_{cc21}|$ (c) of the four-cell common-mode filter. Reprinted with permission from [24]; copyright 2013 PIER.

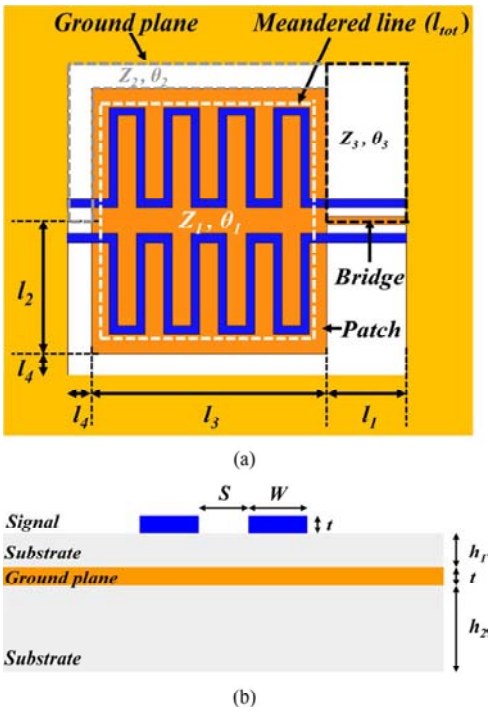

Figure 12. Topology (a) and cross section (b) of the C-shaped patterned ground structure common-mode stopband filter. Reprinted with permission from [17]; copyright 2014 IEEE.

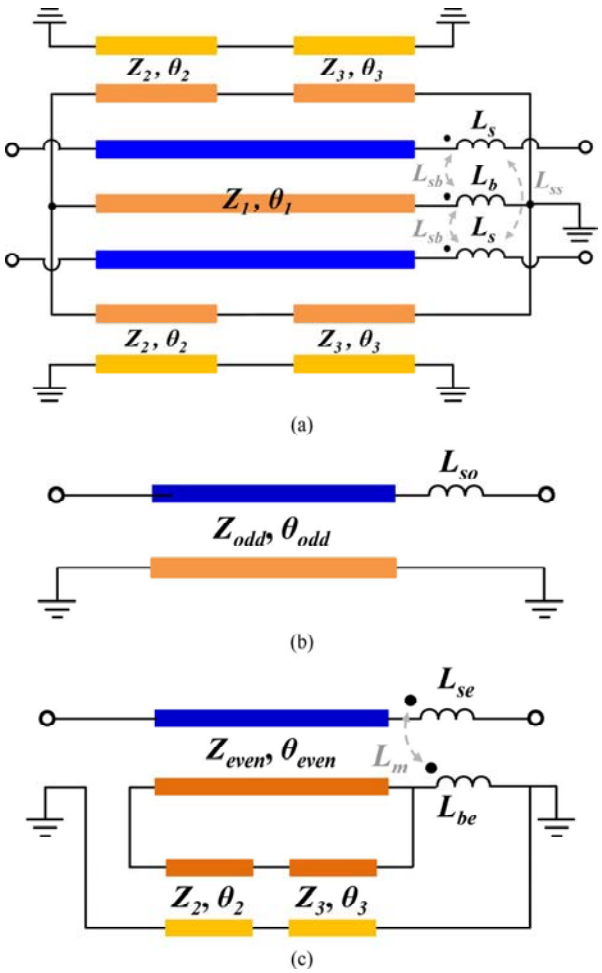

$$L_{so} = L_s - L_{ss}$$
$$L_{se} = L_s + L_{ss} - L_{sb}$$
$$L_{be} = 2L_b - L_{sb}$$
$$L_m = L_{sb}$$

Figure 13. (a) Equivalent circuit model of the common-mode filter of Fig. 12; (b) differential-mode circuit; (c) common-mode circuit. Reprinted with permission from [17]; copyright 2014 IEEE.

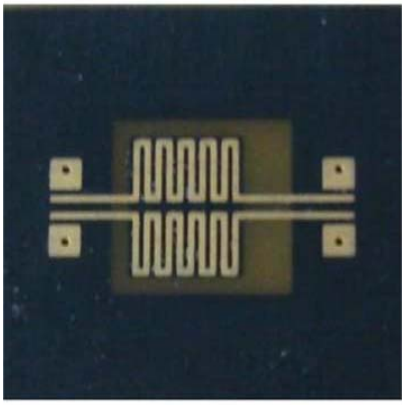

(a)

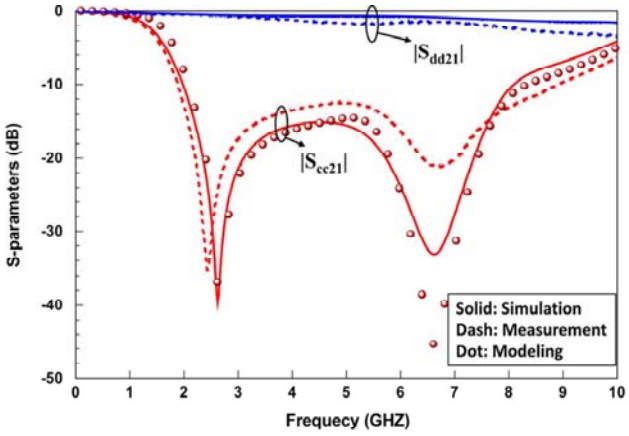

(b)

Figure 14. Photograph (a) and frequency response (b) of the C-shaped patterned ground plane common-mode filter. Reprinted with permission from [17]; copyright 2014 IEEE.

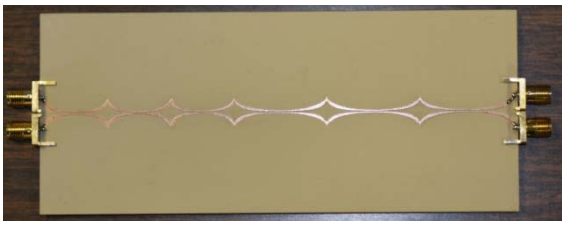

(a)

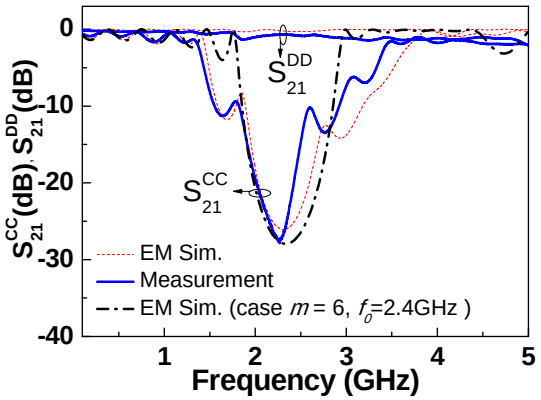

(b)

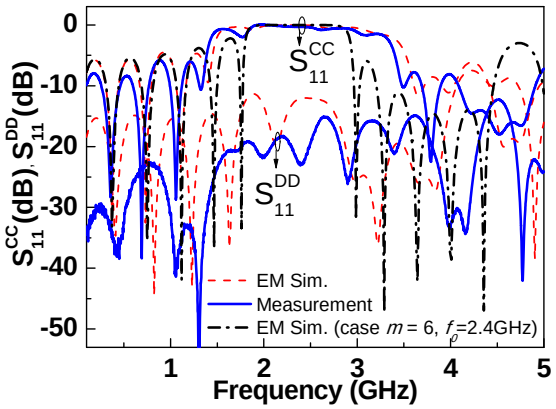

(c)

Figure 15. Photograph (a), differential and common-mode insertion (b) and return (c) loss of the 6-cells non-uniform transmission line based on EBGs with different periods. Reprinted with permission from [41]; copyright 2015 IEEE.

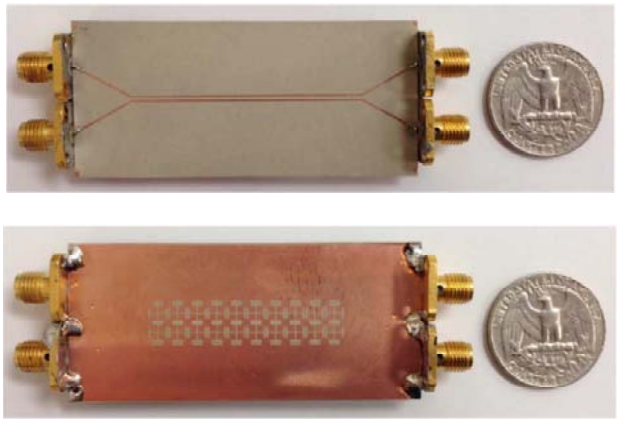

(a)

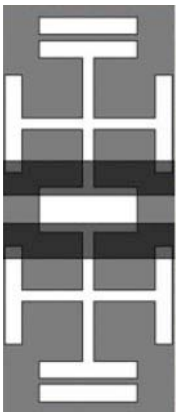

(b)

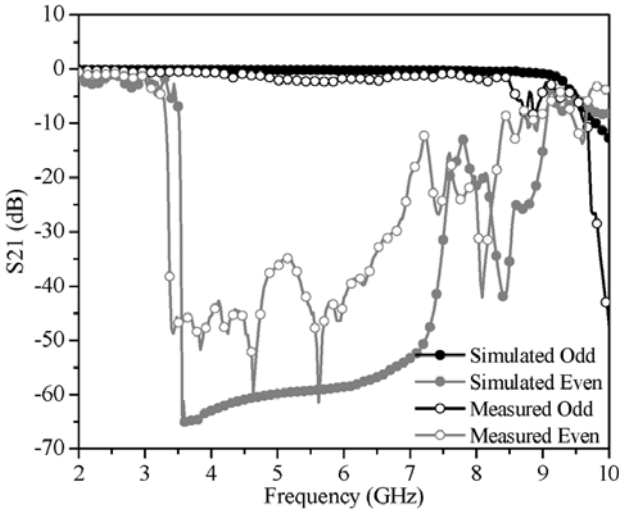

(c)

Figure 16. Photograph of the UC-PBG common-mode stop band filter (a), zoom view of the unit cell (b), and frequency response (c). Reprinted with permission from [40]; copyright 2014 IEEE.